Nucleic Acids Research, 1994, Vol. 22, No. 19 3977–3982

Comparison of antiparallel A·AT and T·AT triplets within an alternate strand DNA triple helix

Elinor Washbrook and Keith R.Fox*
Department of Physiology and Pharmacology, University of Southampton, Bassett Crescent East, Southampton SO9 3TU, UK

Received May 11, 1994; Revised and Accepted August 15, 1994

ABSTRACT

We have examined the formation of alternate strand triple-helices at the target sequence $A_{11}(TC)_6\cdot(GA)_6T_{11}$ using the oligonucleotides $T_{11}(AG)_6$ and $T_{11}(TG)_6$, by DNase I footprinting. These third strands were designed so as to form parallel T·AT triplets together with antiparallel G·GC and A·AT or T·AT triplets. We find that, although both oligonucleotides yield clear footprints at similar concentrations (0.3 μM) in the presence of manganese, only $T_{11}(TG)_6$ forms a stable complex in magnesium-containing buffers, albeit at a higher concentration (10–30 μM). Examination of the interaction of $(AG)_6$ and $(TG)_6$ with half the target site confirmed that the complex containing A·AT triplets was only stable in the presence of manganese. In contrast no binding of $(TG)_6$ was detected in the presence of either metal ion, suggesting that the reverse-Hoogsteen T·AT triplet is less stable that G·GC. We suggest that, within the context of G·GC triplets, the rank order of antiparallel triplet stability is A·AT (Mn^{2+}) > T·AT (Mn^{2+}) > T·AT (Mg^{2+}) > A·AT (Mg^{2+}). Third strands containing a single base substitution in the centre of either the parallel or antiparallel portion showed a (10-fold) weaker interaction in manganese-containing buffers, and no interaction in the presence of magnesium.

INTRODUCTION

The formation of intermolecular DNA triple helices offers the possibility of achieving precise sequence recognition, and has potential for antigene therapy (1,2). The first studies on these structures examined the properties of three-stranded polynucleotides such as poly(A).poly(U).poly(U) (3–5). More recent work has investigated the formation of short intermolecular triplexes by a variety of techniques including affinity cleavage, footprinting and NMR (6–13). Several DNA triplets have been characterized which fall into two distinct classes, depending on the orientation of the third strand, and are illustrated in Figure 1b. In the most widely studied type of triplex, the third strand consists largely of pyrimidines and runs parallel to the purine strand of the target duplex (6,7). Within this motif the best characterized triplets are T·AT and C+·GC (6,7,13), though others including G·TA (14,15) and G·GC (16) have also been described. The requirement for protonation of the third strand cytosine means that triplexes which contain several C·GC triplets are only stable at low pH (<6.0). In the second class of triplex the third strand runs antiparallel to the duplex purine strand and is generally purine-rich (17–21). The best characterized triplets within this motif are G·GC, A·AT and T·AT (11,12,17–21). Since these triplexes are stable at physiological pHs they have been the subject of several studies.

A limitation of either type of triplex is that complex formation is achieved only by recognition of the duplex purine strand, thereby restricting the target sequences to homopurine·homopyrimidine stretches. One way to overcome this limitation is to design triplexes which incorporate both types of motif, achieving recognition of purines on either DNA strand (22–25). However, the formation of these alternate strand triplexes is not facile since the third strand has to alternate across the DNA major groove (22). As a result recognition across R_mY_n junctions is easier than across Y_nR_m (22).

Within the antiparallel (purine-rich) portion of these hybrid triplexes guanines are recognized by the formation of G·GC triplets. However, recognition of adenine can in theory be achieved with either A·AT or T·AT triplets. Although the earliest studies with the antiparallel triplex used A·AT triplets there are several problems concerning its formation. First, work with synthetic polynucleotides suggested that the formation of polydA.polydA.polydT is critically dependent on the length of the strands; only long regions are stable (26). Secondly, some footprinting studies have failed to detect formation of blocks of A·AT triplets (27). Thirdly, it has been suggested that A·AT triplets are sensitive to the nature of the divalent metal ion and are stabilized by manganese or cobalt rather than magnesium (28). In contrast there have been fewer studies on the antiparallel T·AT triplet, and most of these have used a few such triplets interspersed between G·GC triplets so that it might be argued that the complexes are dominated by G·GC triplets (11). Indeed, by using short acridine-linked oligonucleotides designed to form blocks of T·AT triplets, we have recently suggested that T·AT is less stable than G·GC (29).

*To whom correspondence should be addressed

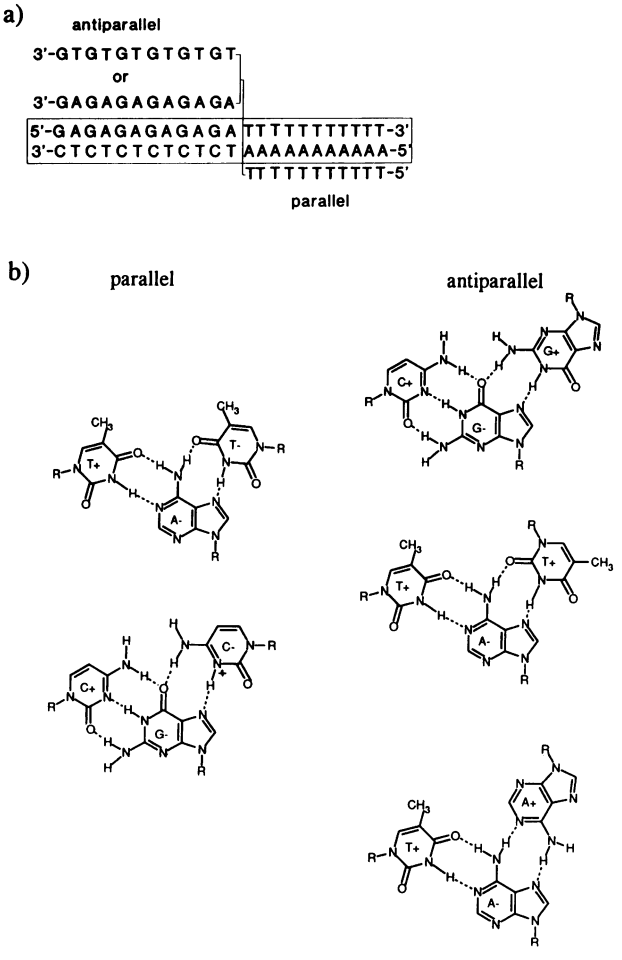

Figure 1. (**a**) Schematic representation of the triplexes formed between $T_{11}(AG)_6$ or $T_{11}(TG)_6$ and the target sequence $(GA)_6T_{11}\cdot A_{11}(TC)_6$. The right hand portion consists of parallel T·AT triplets, while the left-hand segment contains antiparallel G·GC and A·AT or T·AT triplets. (**b**) Structure of parallel (T·AT and C^+·GC) and antiparallel (G·GC, A·AT and T·AT) triplets.

In order to design the optimal oligonucleotide for targeting any particular sequence it will be necessary to know when to use A·AT or T·AT triplets. The present study addresses this question and arises out of our studies on the formation of alternate strand triple helices at the target sequence $A_{11}(TC)_6\cdot(GA)_6T_{11}$. In our initial studies we used the third strand oligonucleotide $T_{11}(AG)_6$, designed to generate a block of parallel T·AT triplets adjacent to an antiparallel triplex consisting of G·GC and A·AT triplets (see Figure 1a). Since our first experiments with this oligonucleotide were unsuccessful, we examined the formation of structures containing antiparallel T·AT triplets in place of A·AT using the third strand oligonucleotide $T_{11}(TG)_6$.

MATERIAL AND METHODS

Oligonucleotides

Oligonucleotides were purchased from Genosys Biotechnologies, Cambridge, UK. These were used without further purification and were dissolved in water at a concentration of 1 mM and stored at −20°C.

DNA plasmids

The oligonucleotides $(GA)_6T_{11}$ and $A_{11}(TC)_6$ were treated with polynucleotide kinase and cloned into *Sma*I cut, alkaline phosphatase treated pUC18 (Pharmacia). Successful clones were picked from X-gal, IPTG containing agar plates as white colonies in the usual way. The sequences were confirmed by DNA sequencing using a T7 sequencing kit (Pharmacia). The insert was oriented so that sequencing with universal primer visualized the sequence $(GA)_6T_{11}$, i.e labelling the 3′ end of the *Hin*dIII strand, used in footprinting studies visualizes the strand containing the sequence $A_{11}(TC)_6$.

DNA fragments

The polylinker fragment containing the insert was obtained by digesting with *Hin*dIII, labelling at the 3′ end with α-(^{32}P)dATP using reverse transcriptase, and cutting again with *Eco*RI. The radiolabelled fragment of interest was separated from the remainder of the plasmid on an 8% polyacrylamide gel. The DNA fragment was labelled on the opposite strand by reversing the order of addition of *Hin*dIII and *Eco*RI.

DNase I footprinting

DNase I footprinting was performed as previously described (25,27,29). Radiolabelled DNA (4 μl), dissolved in 10 mM Tris−HCl pH 7.5 containing 0.1 mM EDTA, was mixed with 4 μl oligonucleotide, diluted in 10 mM Tris−HCl pH 7.5 containing 10 mM NaCl and either 5 mM $MgCl_2$ or 5 mM $MnCl_2$, and left to equilibrate for at least 30 min. The complexes were digested with 2 μl DNase I at 0.01 units/ml and samples were removed at 1 and 5 min and stopped by adding 4 μl formamide containing 10 mM EDTA. In experiments examining the concentration dependence in more detail, only 1 min digestion samples were prepared.

Gel electrophoresis

Products of DNase I digestion were resolved on 10% (for *Hin*dIII labelled fragments) or 13% (for *Eco*RI labelled fragments) polyacrylamide gels containing 8 M urea. 40 cm gels (0.3 mm thick) were run at 1500 V for about 2 h. These were then fixed in 10% acetic acid, dried under vacuum at 80°C and exposed to autoradiography at −70°C using an intensifying screen. Bands in the digest were assigned by comparison with Maxam−Gilbert markers for guanine or guanine and adenine.

Thermal denaturation studies

DNA melting profiles were determined using a Shimadzu UV-2101PC spectrophotometer fitted with a Shimadzu temperature controller (model SPR-8). Heating was applied at 1°C/min in the range 5−90°C with sampling at 0.15°C intervals (eight samples per minute). Data analysis was according to the method of Jones *et al.* (30). T_ms were estimated at the 50% transition point for optical absorption at 260 nm. Triplex melting curves were measured at approximately 5 μM duplex concentration in the presence of a fivefold excess of the third strand.

RESULTS

We have examined the formation of alternate-strand DNA triplexes at the target sequence $A_{11}(TC)_6\cdot(GA)_6T_{11}$ using the oligonucleotides $T_{11}(AG)_6$ and $T_{11}(TG)_6$. These were designed

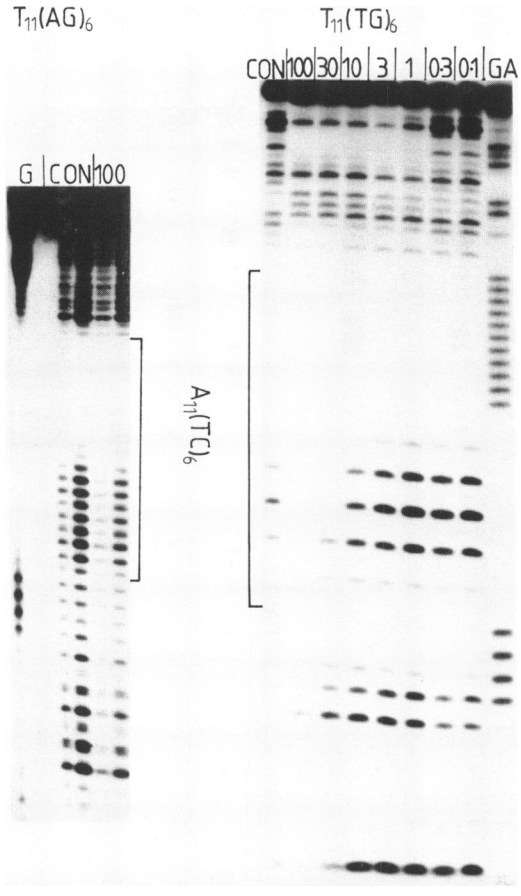

Figure 2. DNase I footprinting patterns for several oligonucleotides on the target sequence $A_{11}(TC)_6 \cdot (GA)_6T_{11}$, obtained at pH 7.5 in the presence of 5 mM $MgCl_2$. The DNA is labelled at the 3′ end of the *Hin*dIII site. For $T_{11}(AG)_6$ each pair of lanes represents digestion by the enzyme for 1 and 5 min, whereas for $T_{11}(TG)_6$ each lane corresponds to digestion by the enzyme for 1 min. Oligonucleotide concentrations (μM) are shown at the top of each pair of lanes. 'CON' indicates the controls. The square brackets indicate the position an length of the triplex target sites. Tracks labelled 'G' and 'GA' are Maxam–Gilbert dimethyl sulphate–piperidine and formic acid–piperidine markers specific for guanine and purines respectively.

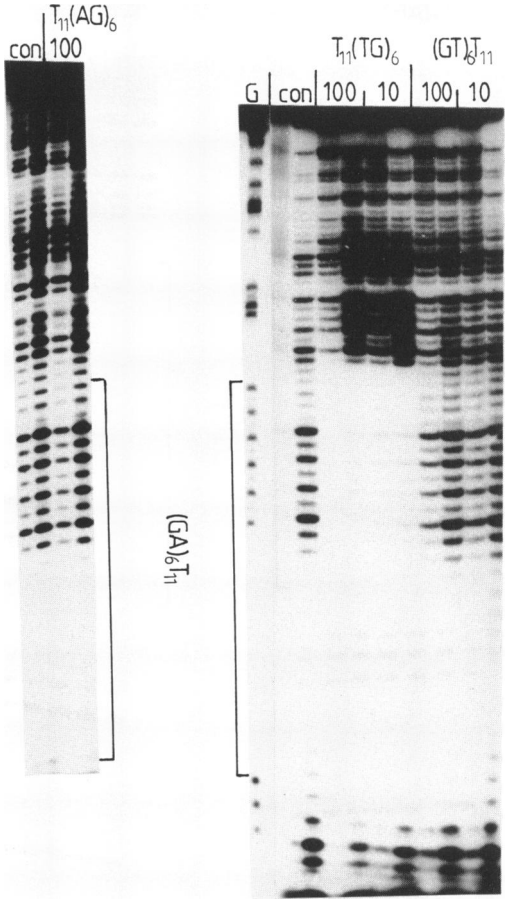

Figure 3. DNase I footprinting patterns for several oligonucleotides on the target sequence $A_{11}(TC)_6 \cdot (GA)_6T_{11}$, obtained at pH 7.5 in the presence of 5 mM $MgCl_2$. The DNA is labelled at the 3′ end of the *Eco*RI site. Other details are as for Figure 1.

to form Hoogsteen (parallel) T·AT triplets with the $T_{11} \cdot A_{11}$ region, together with antiparallel G·GC and either A·AT or T·AT triplets with $(GA)_6 \cdot (TC)_6$ (see Figure 1a). The results of DNase I footprinting experiments performed on complexes formed in magnesium-containing buffers are presented in Figures 2 and 3. Figure 2 shows the fragment labelled at the 3′ end of the *Hin*dIII site (revealing the sequence $A_{11}(TC)_6$), while Figure 3 shows the DNA labelled at the 3′ end of the *Eco*RI site (revealing the sequence $(GA)_6T_{11}$). It can be seen that in both cases the oligonucleotide $T_{11}(AG)_6$, designed to generate a complex containing A·AT triplets, does not affect the DNase I cleavage pattern, even at concentrations as high as 100 μM. In contrast, $T_{11}(TG)_6$ yields clear footprints which extend over the entire length of the insert. This oligonucleotide differs from the previous sequence by replacing the third strand adenines with thymines, thereby enabling the formation of T·AT triplets in the purine-rich (antiparallel) portion. No changes are observed with the control oligonucleotide $(GT)_6T_{11}$ (Figure 3), which has the wrong orientation to form a stable triplex. Examination of the concentration dependence of the changes (Figure 2) reveals that relatively high concentrations of the oligonucleotide (10–30 μM) are required to produce a clear footprint.

Since recent studies have reported that the formation of some triple helices may be critically dependent on the nature of the divalent cation (28), and that A·AT is stabilized by Mn^{2+} rather than Mg^{2+}, we have repeated these experiments in the presence of 5 mM $MnCl_2$. The results are presented in Figures 4 and 5 for the DNA fragment labelled at either end. Looking first at Figure 4, for DNA labelled at the 3′ end of the *Hin*dIII site (visualizing the strand $A_{11}(TC)_6$) it can be seen that, under these conditions, both $T_{11}(AG)_6$ and $T_{11}(TG)_6$ produce clear footprints which persist to concentrations as low as 0.3 μM. It appears that replacing Mg^{2+} with Mn^{2+} has enabled the binding of the oligonucleotide designed to form A·AT triplets. In addition the binding of $T_{11}(TG)_6$ is improved by 30–100-fold in the presence of manganese. Figure 5, in which the DNA is labelled at the *Eco*R1 end, reveals similar footprints for both oligonucleotides and shows that no footprints are produced by the control oligonucleotide $(GT)_6T_{11}$, which has the wrong orientation to form a triplex. Similarly, no changes are produced by $(CT)_6A_{11}$ (not shown) under these conditions; this could in theory form an alternate strand triplex involving antiparallel

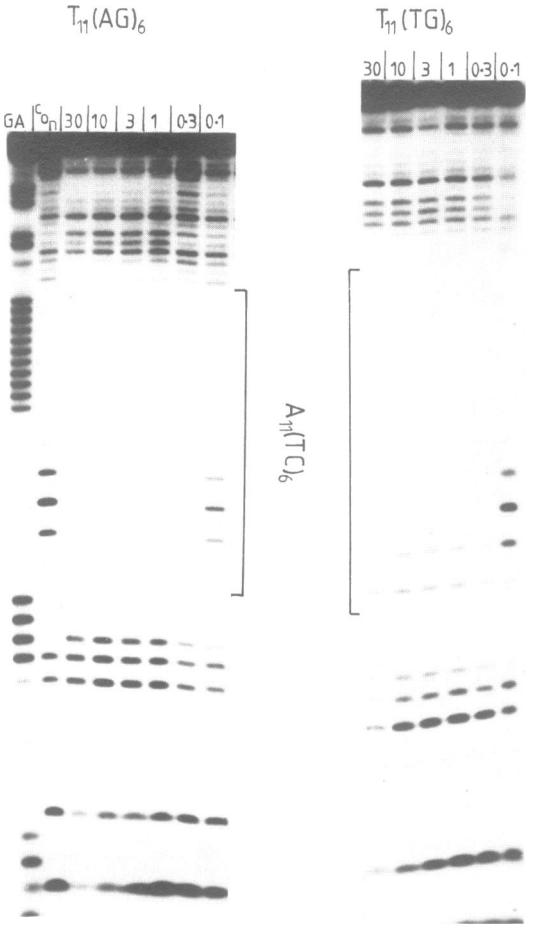

Figure 4. DNase I footprinting patterns for several oligonucleotides on the target sequence $A_{11}(TC)_6 \cdot (GA)_6T_{11}$, obtained at pH 7.5 in the presence of 5 mM $MnCl_2$. The DNA is labelled at the 3′ end of the *Hin*dIII site. Each pair of lanes corresponds to digestion by the enzyme for 1 and 5 min. All other details are as for Figure 2.

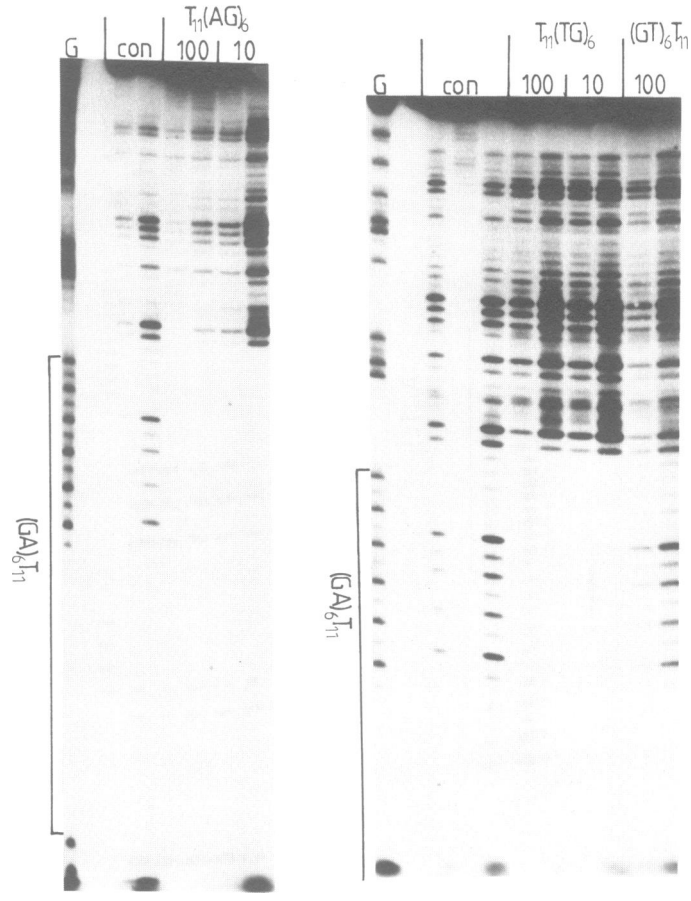

Figure 5. DNase I footprinting patterns for $T_{11}(AG)_6$ and $T_{11}(TG)_6$ on the target sequence $A_{11}(TC)_6 \cdot (GA)_6T_{11}$, obtained at pH 7.5 in the presence of 5 mM $MnCl_2$. The DNA is labelled at the 3′ end of the *Eco*RI site. Oligonucleotide concentrations (μM) are shown at the top of each lane, which corresponds to digestion by the enzyme for 1 min. All other details are as for Figure 2.

A·AT and parallel T·AT and C^+·GC triplets which should only be stable at low pH.

We have previously shown that, as well as increasing the binding of the correct oligonucleotides, manganese can also stabilize complexes containing triplex mismatches (25). We were therefore concerned that the increased binding observed in the presence of manganese might represent a non-specific effect. It is clear that some considerable specificity must be retained since the footprints are still restricted to the target regions of interest; DNase I cleavage of the remainder of the fragment is unaffected. We have examined the effect of single triplet mismatches on the formation of these triplexes by studying the interaction of $T_5AT_5(TG)_6$ and $T_{11}(TG)_3GG(TG)_2$ with the same target site. The former generates a single A·AT mismatch in the centre of the block of parallel T·AT triplets, while the latter forms a G·AT triplet in the centre of the antiparallel portion. Neither of these are canonical base triplets. We find that neither oligonucleotide produces a DNase I footprint in magnesium-containing buffers. In contrast Figure 6 shows the footprinting patterns produced in the presence of manganese. It can be seen that both oligonucleotides do induce footprints, at concentrations of 3 μM and above, in contrast to the correct oligonucleotides ($T_{11}(TG)_6$ and $T_{11}(AG)_6$) which produce footprints at 0.5 μM. However, the region affected is different for the two oligonucleotides. $T_5AT_5(TG)_6$ (generating a mismatch in the upper $T_{11} \cdot A_{11} \cdot T_{11}$ portion) produces a footprint which is at least 2−3 bases shorter in the upper (5′) direction than $T_{11}(TG)_6$. With the correct oligonucleotide the footprint extends beyond the upper end of the target site by 2−3 bases, whereas with there is no protection in this region with the mismatch oligonucleotide. Since DNase I cleavage of the A_{11} region is extremely poor in the control, we cannot estimate the precise change in the site size, though the shorter footprint suggests that the terminal portion, beyond the mismatch, is not interacting with the target site. The pattern at the 3′ (lower) end is similar to that produced by $T_{11}(TG)_6$. Since $(TG)_6$ alone does not interact with this target site (see below), the T_5AT_5 portion must impart some additional stability to the complex, though it is not clear whether this results from all 11 bases or merely from the five closest to the centre, after the mismatched A residue. With $T_{11}(TG)_3GG(TG)_2$ the pattern at the upper end of the target is similar to that with $T_{11}(TG)_6$. However, in this instance some bands are still evident at the lower end of the target site (especially noticeable with 3 μM oligonucleotide); this difference occurs at the end containing the third strand mismatch. It may be significant that $T_5AT_5(TG)_6$

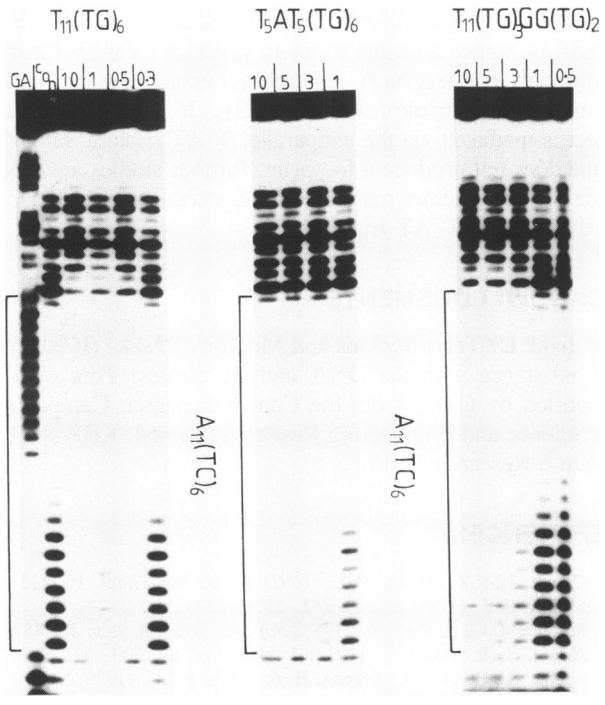

Figure 6. DNase I footprinting patterns for oligonucleotides containing single triplet mismatches in either half of the third strand. The experiment was performed at pH 7.5 in the presence of 5 mM $MnCl_2$. The DNA is labelled at the 3′ end of the *Hin*dIII site. Oligonucleotide concentrations (μM) are shown at the top of each lane, which corresponds to digestion by the enzyme for 1 min. The track labelled 'con' is a control. The square brackets show the position and length of the target site. The track labelled 'GA' is a Maxam–Gilbert formic acid–piperidine marker specific for purines.

Table 1. Melting point transitions for the duplex $A_{11}(TC)_6 \cdot (GA)_6T_{11}$ in the presence and absence of the oligonucleotides $T_{11}(AG)_6$ and $T_{11}(TG)_6$.

	Mg^{2+}	Mn^{2+}
$A_{11}(TC)_6 \cdot (GA)_6T_{11}$ duplex	61	60
$A_{11}(TC)_6 \cdot (GA)_6T_{11}$ + $T_{11}(AG)_6$	27, 61	34, 62
$A_{11}(TC)_6 \cdot (GA)_6T_{11}$ + $T_{11}(TG)_6$	27, 61	38, 58

These were determined as described in the Methods section in 10 mM Tris–HCl pH 7.5 containing 10 mM NaCl and, 5 mM $MgCl_2$ or 5 mM $MnCl_2$.

produces a footprint at a slightly lower concentration than $T_{11}(TG)_3GG(TG)_2$ (bands in the former have not completely returned to the intensity of the control at 1 μM, whereas in the latter they begin to reappear at 3 μM), suggesting that a G·AT mismatch within the antiparallel portion has a greater effect than an A·AT mismatch within the parallel half of the alternate strand triplex.

We have extended the studies on the stability of these triple helices by examining the thermal denaturation profiles of the oligonucleotides under similar conditions. The results are summarized in Table 1. It can be seen that the nature of the divalent cations (magnesium or manganese) has little or no effect on the stability of the duplex $(GA)_6T_{11} \cdot A_{11}(TC)_6$. Melting profiles in the presence of the third strands revealed an additional

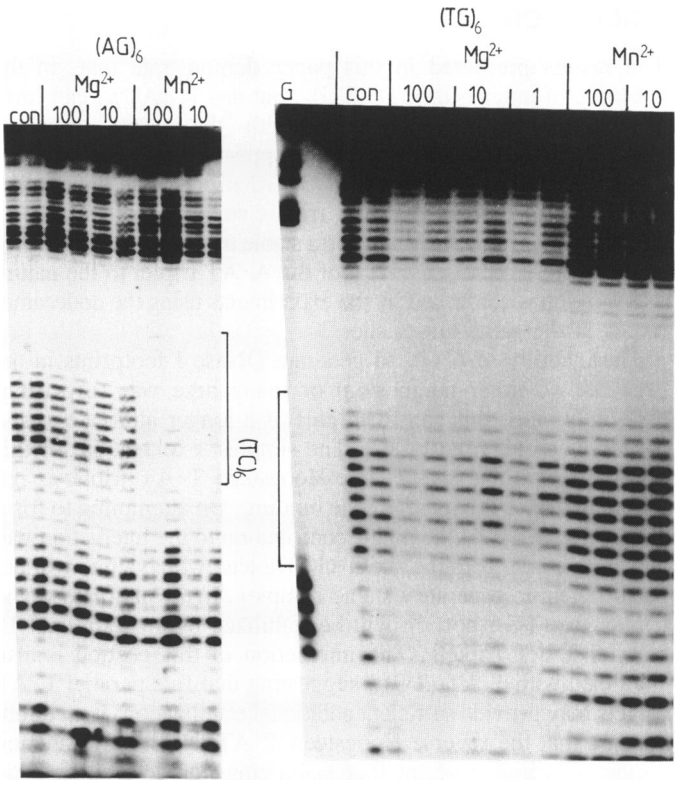

Figure 7. DNase I digestion of the fragment containing the insert $A_{11}(TC)_6 \cdot (GA)_6T_{11}$ in the presence of $(TG)_6$ and $(AG)_6$. The DNA is labelled at the 3′ end of the *Hin*dIII site. The complexes were prepared in 10 mM Tris-HCl containing either 5 mM $MgCl_2$ or 5 mM $MnCl_2$. Each pair of lanes corresponds to digestion by the enzyme for 1 and 5 min. Oligonucleotide concentrations (μM) are shown at the top of each pair of lanes. The tracks labelled 'con' are controls, performed in the presence of 5 mM $MnCl_2$, but no oligonucleotides. The square brackets show the position of the $(TC)_6$ sequences. The tracks labelled 'G' is a dimethyl sulphate-piperidine marker specific for guanine.

broad transition between 10 and 40°C, with no effect on the melting of the duplex. Although triplex transitions were observed for $T_{11}(TG)_6$ and $T_{11}(AG)_6$ in both Mn^{2+} and Mg^{2+}, these were increased by 11°C ($T_{11}(TG)_6$) and 7°C ($T_{11}(AG)_6$) in the presence of Mn^{2+}.

The footprinting results suggest that, in the presence of magnesium, the antiparallel T·AT triplet imparts a greater stability to the alternate strand triplex than A·AT, whereas both triplets are stable in manganese-containing buffers. In order to demonstrate that this is caused by the triplets themselves, and is not due to some unusual property of alternate-strand structure, we have examined the interaction of $(TG)_6$ and $(AG)_6$ with the $(GA)_6 \cdot (TC)_6$ portion of the same fragment. The results are presented in Figure 7. Looking first at $(AG)_6$ it can be seen that, as expected, this produces a clear footprint in the presence of manganese, but shows no interaction when the divalent cation is magnesium. It therefore appears that the inability of $T_{11}(AG)_6$ to form an alternate strand triplex in the presence of magnesium arises from instability of the A·AT triplet under these conditions. In contrast, $(TG)_6$ does not generate a footprint at this target site with either magnesium or manganese, even at oligonucleotide concentrations as high as 100 μM.

DISCUSSION

The results presented in this paper demonstrate that, in the presence of magnesium, $T_{11}(TG)_6$, but not $T_{11}(AG)_6$, can form an intermolecular triple helix with the target sequence $(GA)_6T_{11}\cdot A_{11}(TC)_6$. It therefore appears that, under these conditions and in the context of G·GC triplets, the antiparallel T·AT triplet imparts a greater triplex stability than A·AT. In contrast both oligonucleotides form stable triplexes in the presence of manganese. The sensitivity of the A·AT triplet to the nature of the cation is confirmed by the experiments using the dodecamer $(AG)_6$ at the same target site.

The inability of $(TG)_6$ to generate DNase I footprints in the presence of either magnesium or manganese was surprising, especially since this can form part of a longer alternate strand triplex when tethered to T_{11}. The simplest explanation for this observation is that the reverse-Hoogsteen T·AT triplet is not strong and does not augment the binding. On attempting to form a triplex with $(TG)_6$ the major contribution to the interaction will therefore come from the six G·GC triplets, which alone will not be sufficient to generate a stable complex. In the alternate strand triplex the $(TG)_6$ portion will be stabilized by an additional 11 parallel T·AT triplets. The interaction of this portion is also stabilized with $T_5AT_5(TG)_6$, suggesting that five parallel T·AT triplets may provide sufficient additional stabilization. It therefore appears that the reverse Hoogsteen T·AT triplet may function almost as a null base, neither stabilizing nor destabilizing the complex, only making a small contribution to the interaction. The lower stability of this triplet is consistent with recent work using acridine-linked oligonucleotides, which failed to detect complex formation between 5′-Acr-T_5G_5 and the target $G_6A_6\cdot T_6C_6$ (29).

This contrasts with the triplexes containing A·AT triplets. No interaction was detected between $(AG)_6$ and $(TC)_6\cdot(GA)_6$ in the presence of magnesium, even when it was tethered to T_{11} to form the alternate strand structure. Although the 11 parallel T·AT triplets stabilize the interaction of $(TG)_6$ with $(TC)_6\cdot(GA)_6$ these are not sufficient to stabilize the interaction with $(AG)_6$. It therefore appears that, in the presence of magnesium, the potential A·AT triplets destabilize the complex. However, addition of manganese appears to stabilize the A·AT triplets so that $(AG)_6$ alone generates a triplex. On the basis of these results it seems that, within the context of G·GC triplets, the rank order of antiparallel triplet stability is A·AT (Mn^{2+}) > T·AT (Mn^{2+}) > T·AT (Mg^{2+}) > A·AT (Mg^{2+}).

It is worth noting that, according to the model for alternate strand formation across an RY junction, the central two base pairs will be skipped by the third strand (22,25). As a result only 21 triplets will be formed along the 23 base pair target region. Each of the 23-mer oligonucleotides could therefore bind in several positions, depending on which two base pairs across the junction are omitted (i.e. GA, AT or TT). The present studies do not provide information on the precise location of the third strand oligonucleotides and it is possible that this may be different for the magnesium and manganese complexes.

The present studies confirm previous reports that manganese stabilizes the antiparallel A·AT triplet (28). There is at least a 100-fold difference in the concentration of $T_{11}(AG)_6$ required to generate a footprint between magnesium and manganese (compare 0.3 μM with > 100 μM). Although we have previously shown that manganese can stabilize some triplet mismatches (25), this cannot be a totally non-specific effect, since the deliberate introduction of other mismatches further destabilizes the structure, requiring higher concentrations to produce clear footprints. In addition to its effect on A·AT triplets, manganese facilitates the formation of a triplex with $T_{11}(TG)_6$. It is unlikely that this effect is mediated via the antiparallel T·AT triplets, since $(TG)_6$ alone does not produce a footprint. Further studies are required to determine whether manganese acts via the antiparallel G·GC or the parallel T·AT triplets.

ACKNOWLEDGEMENTS

We thank Dr Terry Jenkins and Mr Tony Reszka (ICR, Sutton) for assistance with the DNA melting curves. This work was supported by grants from the Cancer Research Campaign and the Science and Engineering Research Council. KRF is a Lister Institute Research Fellow.

REFERENCES

1. Chubb, J.M. & Hogan, M.E. (1992) *Trends Biotechnol.* **10**, 132–136.
2. Moffat, A.S. (1991) *Science* **252**, 1374–1375.
3. Felsenfeld, G. & Rich, A. (1957) *Biochim. Biophys. Acta* **26**, 457–468.
4. Arnott, S. & Selsing, E. (1974) *J. Mol. Biol.* **88**, 509–521.
5. Arnott, S., Bond, P.J., Selsing, E. & Smith, P.J.C. (1976) *Nucleic Acids Res.* **11**, 4141–4155.
6. Moser, H.E. & Dervan, P.B. (1987) *Science* **238** 645–650.
7. LeDoan, T., Perroualt, L., Praseuth, D., Habhoub, N., Decout, J.L., Thoung, N.T., Lhomme, J. & Hélène, C. (1987) *Nucleic Acids Res.* **15**, 7749–7760.
8. Thuong, N.T. & Hélène, C. (1993) *Angewandte Chemie* **32**, 666–690.
9. Sun, J.-S. & Hélène, C. (1993) *Curr. Opin. Struct. Biol.* **3**, 345–356.
10. Hélène, C. (1993) *Curr. Opin. Biotechnol.* **4**, 29–36.
11. Radhakrishnan, I., de los Santos, C. & Patel, D.J. (1993) *J. Mol. Biol.* **234**, 188–197.
12. Radhakrishnan, I. & Patel, D.J. (1993) *Structure* **1**, 135–152.
13. Radhakrishnan, I. & Patel, D.J. (1994) *Structure* **2**, 17–32.
14. Wang, E., Malek, S. & Feigon, J. (1992) *Biochemistry* **31**, 4838–4846.
15. Griffin, L.C. & Dervan, P.B. (1989) *Science* **245**, 967–971.
16. Giovannangeli, C., Rougée, M., Garestier, T., Thuong, N.T. & Hélène, C. (1992) *Proc. Natl Acad. Sci. USA* **89**, 8631–8635.
17. Beal, P.A., & Dervan, P.B. (1991) *Science* **251**, 1360–1363.
18. Chen, F.-M. (1991) *Biochemistry* **30**, 4472–4479.
19. Pilch, D.S., Levenson, C. & Shafer, R.H. (1991) *Biochemistry* **30**, 6081–6087.
20. Beal, P.A. & Dervan, P.B. (1992) *Nucleic Acids Res.* **20**, 2773–2776.
21. Durland, R.H., Kessler, D.J., Gunnell, S., Duvic, M., Pettott, B.M. & Hogan, M.E. (1991) *Biochemistry* **30**, 9246–9255.
22. Beal, P.A & Dervan, P.B. (1992) *J. Am. Chem. Soc.* **114**, 4976–4982.
23. Jayasena, S. & Johnston, B.H. (1992) *Biochemistry* **31**, 320–327.
24. Jayasena, S.D. & Johnston, B.H. (1992) *Nucleic Acids Res.* **20**, 5279–5288.
25. Washbrook, E. & Fox, K.R. (1994) *Biochem. J.* **301**, 569–575.
26. Broitman, S.L., Im, D.D. & Frezco, J.R. (1987) *Proc. Natl Acad. Sci. USA* **84**, 5120–5124.
27. Chandler, S.P. & Fox, K.R. (1993) *FEBS Lett.* **332**, 189–192.
28. Malkov, V.A., Voloshin, O.N., Soyfer, V.N. & Frank-Kamenetskii, M.D. (1993) *Nucleic Acids Res.* **21**, 585–591.
29. Fox, K.R. (1994) *Nucleic Acids Res.* **22**, 2016–2021.
30. Jones, G.B., Davey, C.L., Jenkins, T.C., Kamal, A., Kneale, G.G., Neidle, S., Webster, G.D. & Thurston, D.E. (1990) *Anti-Cancer Drug Design* **5**, 249–264.